

The effect of sulfide content(x) on the electrical properties of (ZnS_xSe_{1-x}) thin films

R.M.S.Al-Haddad¹, Bushra A.Hasan¹, Majed.A.Dwech²

¹ Department of Physics, College of Science, University of Baghdad,

² Department of Physics, College of Science, University of Kerbala

Abstract

Thin films of ZnS_xSe_{1-x} with different sulfide content(x) (0, 0.02, 0.04, 0.06, 0.8, and 0.1), thickness (t) (0.3, 0.5, and 0.7 μm) and annealing temperature (Ta) (R.T 373 and 423K) were fabricated by thermal evaporating under vacuum of 10⁻⁵ Torr on glass substrate. The results show that the increasing of sulfide content (x) and annealing temperature lead to decrease the d.c conductivity σ_{DC} and concentration of charge carriers (n_H) but increases the activation energy (E_{a1}, E_{a2}), while the increasing of t increases σ_{DC} and n_H but decrease (E_{a1}, E_{a2}). The results were explained in different terms.

Key words

ZnS Thin films,
Hall effect,
Carriers
concentration.

Article info

Received: Nov. 2011

Accepted: Apr. 2012

Published: Oct. 2012

تأثير محتوى الكبريت على الخواص الكهربائية لأغشية ZnS_xSe_{1-x} الرقيقة

رعد محمد صالح الحداد¹، بشرى عباس حسن¹، ماجد حسين دويج²

¹ قسم الفيزياء، كلية العلوم، جامعة بغداد

² قسم الفيزياء، كلية العلوم، جامعة كربلاء

الخلاصة

تم تحضير أغشية رقيقة من ZnS_xSe_{1-x} بنسب مختلفة من المحتوى من الكبريت وبأسماك وبدرجات حرارة تليدين مختلفة بطريقة التبخير الحراري تحت الفراغ على أرضية زجاجية. أظهرت النتائج ان زيادة المحتوى من الكبريت ودرجة حرارة التليدين يؤدي الى نقصان في قيم التوصيلية الكهربائية المستمرة σ_{DC} وكثافة حاملات الشحنة n_H لكنه يزيد قيم طاقة التنشيط E_{a1}, E_{a2} بينما زيادة السمك أدى إلى زيادة قيم كل من σ_{DC} و n_H وهبوط قيم E_{a1}, E_{a2}. فسرت النتائج بدلالة رموز مختلفة.

Introduction

The II-VI wide band gap semiconducting alloys have applications in fabricating technologically important solid state devices [1, 2]. The ZnS_xSe_{1-x} semiconducting alloys are used to fabricate optoelectronic devices ranging from infrared to ultraviolet (UV) radiation [3]. Due to variation in band gap with composition, these are highly suitable to fabricate wavelength tunable UV-photodiodes [4]. Also the direct band gap over entire composition range (0 ≤ x ≤ 1) enables its usage in visible laser diodes, light emitting diodes (LEDs) and bright light emitters [1].

The II-VI mixed-anion semiconductor alloys are studied relatively less than the mixed-cation alloys both from theoretical methods and experimental techniques. A few theoretical models have been applied on ternary alloys and the binary compounds. For instance, Homann et al [5] applied linear combination of atomic orbitals (LCAO) method to report electronic and structural properties of ZnS_xSe_{1-x} alloys over entire composition range. On the basis of EPM, Nasrallah et al [6] reported the electronic structure and band offsets of ZnS_xSe_{1-x} alloys and heterostructures. A semi empirical

MSINDO method was applied by Janetzko and Jug [7] to compute binding energies, entropy of mixing and miscibility of ZnS_xSe_{1-x} . The quasi particle scheme was applied by Fitzer et al [8] for ZnS and ZnSe. A gradient corrected hybrid scheme was employed to report band gap for a number of materials including ZnS by Muscat and coworkers [9]. Bernard and Zunger [10] reported the band gap and related properties of $ZnS_{0.5}Se_{0.5}$ using plane wave method based on local density approximation (LDA).

Only a few experimental studies of the ZnS_xSe_{1-x} alloys are reported. The difficulty posed by miscibility in forming the solid state might probably be the reason for paucity of experimental studies. Nevertheless, very recently Homann et al [5] reported band gap for all compositions applying optical spectroscopy. Thesis [11] reported experimental band gap for the binary compounds ZnS and ZnSe. Ebina et al [12] reported reflectivity measurements and indicated that ZnS_xSe_{1-x} alloys are amalgamation type.

In this comprehensive study we report the d.c conductivity values of and the concentration of charge carriers, type of conductance, mobility, activation energy for ZnS_xSe_{1-x} prepared with different composition, thickness and annealing temperatures for practical applications. The computed quantities are compared with available experimental data for. The paper is organized as follows: in second section we briefly describe the method of calculation. In III section, we discuss and present our results. The fourth section is devoted to conclude findings of this work.

Experimental Part

Appropriate atomic weights of Zn, S and Se with high purity 99.999 % for alloy, and appropriate atomic percentages of high purity ZnS , ZnSe with the resultant of ZnSSe alloy to prepare the films. By

using a sensitive electrical balance type (Mettler H35), all weights of the elements and compound have been weighted and then put in a clean and dry quartz ampoules (ZnS with ZnSe) to get ZnSSe alloy. The constituent were mixed together and then sealed under vacuum of 2×10^{-5} Torr . Then the sealed ampoules were placed in a programmable a furnace type (Heraeus). As indicated the ampoules heated first at (773, 1023, 1173, and 1373) K and kept at this temperature for (20, 20, 20, and 3) hours respectively. With raising the temperature at rate 278K/min.

In the present work thin films of alloys of ZnS_xSe_{1-x} has been synthesized with different x content where (x =0,0.02,0.04,0.06,0.08 and 0.1) and different thickness 0.3,0.5, and 0.7 μ m were prepared using thermal evaporation by continuously feeding the material with a powder to a heated molybdenum boat of melting point where instantaneous evaporation of the material will take place. Corning glass slides substrates were used which were subjected to several cleaning stages, and the distance of the source to substrate was 15cm. The evaporation carried out using Edward coating unit (model E306A) that was evacuated by means of oil-diffusion and rotary pumps. During the evaporation of the films, the pressure in the system was 4×10^{-5} Torr. All the samples were prepared under constant condition: - pressure, substrate temperature (room temperature) and thickness. After the deposition process was ended the current supply was switched off and the samples were lifted in high vacuum for several hours, then the air admitted to the chamber, and the films were taken out from the coating unit and the measurements were made. Finally, all the prepared films thermally treatment under vacuum of 10^{-2} Torr at different temperature (373 and 423K) for one hour. Then the measurements were made.

D.C electrical conductivity of semiconductor (σ) is given by the formula [5]:-

$$\sigma = e(\mu_n \cdot n + \mu_p \cdot p) \quad (1)$$

Where μ_n and μ_p are the mobility of electrons and holes respectively in units of (cm²/V.sec). The n and p are the concentrations of electrons and holes and are measured in units of (cm⁻³) and e is the charge of electron. The change of electrical conductivity with temperature of semiconductors is given by the equation [5]:-

$$\sigma = \sigma_0 e\left(-\frac{E_a}{k_B T}\right) \quad (2)$$

Where E_a is the thermal activation energy, T is the absolute temperature, k_B is the Boltzmann constant and σ_0 is the minimum metallic conductivity (the value of σ when $T \rightarrow \infty$) Hall effect results from applying magnetic field (B_z) along a rectangular sample normal to the direction of current (I), the charge carriers will tend to be deflected to one side, then building up potential gradient perpendicular to magnetic field and current, this effect was used to determine the type and the density of charge carriers (n_H). Hall coefficient (R_H) is given by:-

$$R_H = \frac{V_H \cdot t}{I \cdot B_z} \quad (3)$$

Where t is the film thickness, the density of charge carriers is given by the relation:-

$$R_H = -\frac{1}{n_H e} \quad (4)$$

The mobility of Hall (μ_H) is given by the relation [13] :-

$$\mu_H = \sigma |R_H| \quad (5)$$

Vacuum evaporated aluminum electrodes at the bottom of substrates were previously done for electrical properties

measurements. D.C electrical conductivity measurements were carried out at the temperature range (298-513) K using the electrical circuit which is consists of Oven type Herease, Power supply and Ammeter. The resistivity (ρ) of ZnS_xSe_{1-x} samples deposited at room temperature were obtained using the following equation :-

$$\rho = \frac{Rwt}{L} \quad (6)$$

Where L and w are the length and the width of sample respectively and R and t is the resistivity and thickness of the film, the conductivity of the mentioned samples was obtained from the relation:-

$$\sigma = \frac{1}{\rho} \quad (7)$$

The activation energy (E_a) of the ZnS_xSe_{1-x} samples can be deduced by applying the following relation:-

$$E_a = \text{slop} \times 0.08652 \quad (8)$$

Where:-

$$\text{slop} = \frac{d \ln \sigma}{d(1000/T)} \quad (9)$$

The measurements of the density of charge carriers and the Hall mobility were provided from applying equations (5 and 6) respectively.

Results and Discussion

Figs.1 to 10 show the XRD patterns of $Zn S_x Se_{1-x}$ alloys and vacuum evaporated thin films which were deposited on glass at a room temperature with different S content (0,0.2,0.4,0.6,0.8,and0.1), different thicknesses (0.0,0.5,and 0.7 μ m) and annealed at 373and 423K. It is well known that pure Zn (Se, S) materials exist in two crystalline phases, i. e., a cubic form with sphalerite structure and a hexagonal form with wurtzite structure. The XRD patterns for ternary $Zn S_x Se_{1-x}$ thin films deposited with different thicknesses on glass substrates indicated the polycrystalline nature with zinc blend structure. The X-ray diffractogram of $Zn S_x Se_{1-x}$ thin films showed the $\langle 111 \rangle$,

$\langle 220 \rangle$ and $\langle 311 \rangle$ reflections, of which the intensity of the $\langle 111 \rangle$ orientation is predominant. This study reveals that the alloys and the vacuum evaporated $\text{ZnS}_x\text{Se}_{1-x}$ thin films with different thicknesses on glass substrates are polycrystalline cubic structure. The similar crystalline structures were generally observed for $\text{ZnS}_x\text{Se}_{1-x}$ thin films by [14]. The intensity of the $\langle 111 \rangle$ peak for all prepared thin films decreases as thin film thickness increases. While addition of sulfide causes little shifting of 2θ location to higher values and an increase of the peaks intensity which be more significant at higher S concentration.

The plots of $\ln\sigma$ versus $10^3/T$ for $\text{ZnS}_x\text{Se}_{1-x}$ films in the range (298-513) K at different thicknesses, annealing temperatures and composition are shown in Figs. (11-19). It is clear from these figures that there are two transport mechanisms, giving rise to two activation energies E_{a1} and E_{a2} . The conduction mechanism of the activation energy (E_{a2}) at the higher temperatures range (413-513) K is due to carrier's excitation into the extended states beyond the mobility edge, and the activation energy (E_{a1}) at the lower range of temperatures (298-303) K, the conduction mechanism is due to carrier's excitation into localized state at the edge of the band. Tables (1to3) show the effect of different thickness, annealing temperature and composition on both activation energies E_{a1} and E_{a2} for $\text{ZnS}_x\text{Se}_{1-x}$ films. It is clear that the activation energies decrease with increasing of the thickness but increase with increasing of annealing temperatures and different composition. These results are in agreement with Segui et al [15].

The activation energy E_{a1} for $\text{ZnS}_x\text{Se}_{1-x}$ films for $x=0.0$ at thickness $0.3\mu\text{m}$ increases with increasing of annealing temperature and different composition. It is clear that at $x=0.0$ E_{a1} increases from 0.0258 to 0.0638 eV when the annealing temperature changes from 373 to 423 K and different composition,

while E_{a2} increases from 0.449 to 1.277 eV when annealing temperature changes from 373 to 423 K. Similar behavior of films appears for other thicknesses as shown in Table (1to3), on the other hand the activation energy (E_{a1}) for $\text{ZnS}_x\text{Se}_{1-x}$, at $0.3\mu\text{m}$ thickness increases from 0.0258 to 0.0538 eV when the sulfide concentration x increases from 0 to 0.1. One can observe from the same Tables that E_{a1} and E_{a2} exhibit to change in contrast manner with thickness variation from that with T_a and x , i.e. E_{a1} and E_{a2} decrease with t . It is clear that E_{a1} decreases from 0.0258 to 0.0229 eV at $x=0.0$ for as deposited $\text{ZnS}_x\text{Se}_{1-x}$ thin films, this behavior is an action of approaching the structure of the sample from bulk material as a result of thickness increasing. The increasing in the activation energy with increasing of composition may be due to the increase of the energy gap with the increasing of composition, while the increasing of (E_{a1}, E_{a2}) with T_a resulting from the effect of heat treatment which causes eliminating of states in the band gap consequently the activation energies will be rises.

The type of charge carriers, concentration (n_H) and Hall mobility (μ_H), have been estimated from Hall measurements. The results show that the films of all thicknesses have a negative Hall coefficient (n-type charge carriers), i.e. Hall voltage decrease with increasing the current. Similar results were obtained by Al-Hamed [16]. The variation of Hall mobility with annealing temperatures of $\text{ZnS}_x\text{Se}_{1-x}$ films at different composition are shown in Tables (4-6). We can notice from these figures that both the Hall mobility and carrier concentration decrease with increasing of composition and annealing temperature while they increase with increasing of thickness. This result is in agreement with the result of Al-Hamed [16], and this may be due to either increasing the trapping centers or the films have a large amount of adsorbed

oxygen which reduces both the number of charge carriers and their mobility

essentially because of the higher grain boundary barrier height.

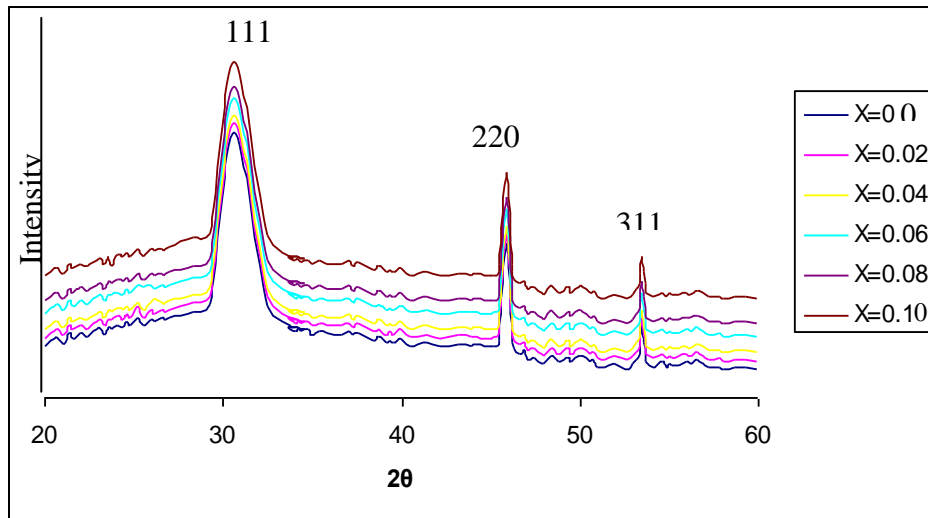


Fig.(1) X-ray pattern for ZnS_xSe_{1-x} (powder).

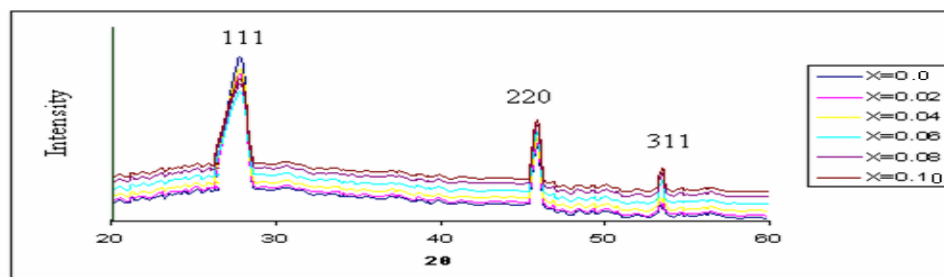


Fig. (2) X- ray pattern for as deposited ZnS_xSe_{1-x} films with thickness $0.3\mu m$.

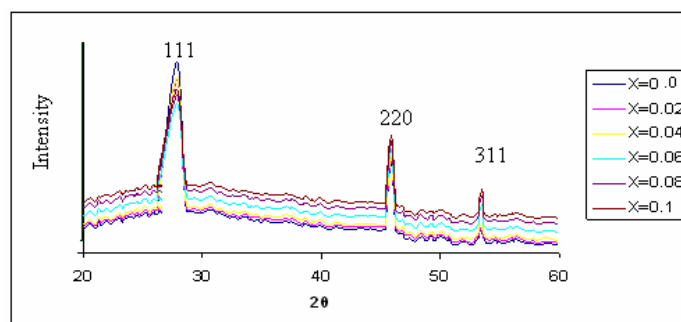


Fig (3) X- ray pattern for as deposited ZnS_xSe_{1-x} films with thickness $0.3\mu m$ annealed at 373 K

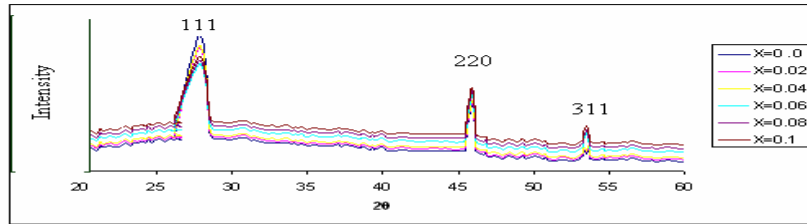


Fig. (4), X- ray pattern for as deposited ZnS_xSe_{1-x} films with thickness 0.3μm annealed at 423 K

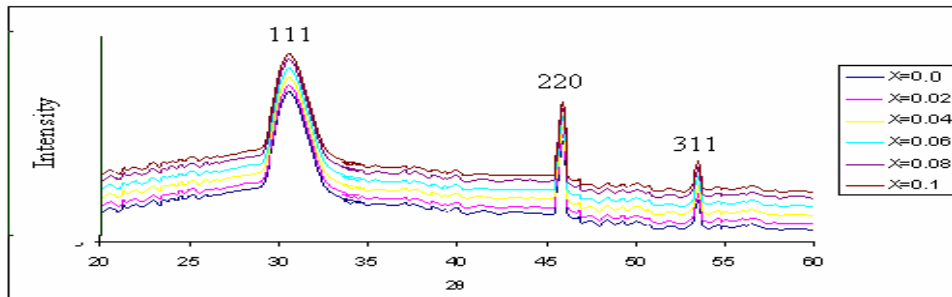


Fig. (5), X- ray pattern for as deposited ZnS_xSe_{1-x} films with thickness 0.5μm.

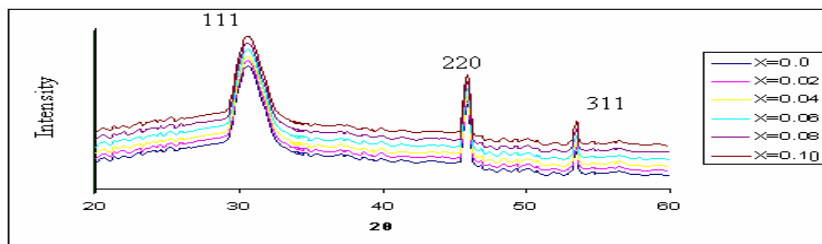


Fig. (6) X- ray pattern for as deposited ZnS_xSe_{1-x} films with thickness 0.5μm annealed at 373 K.

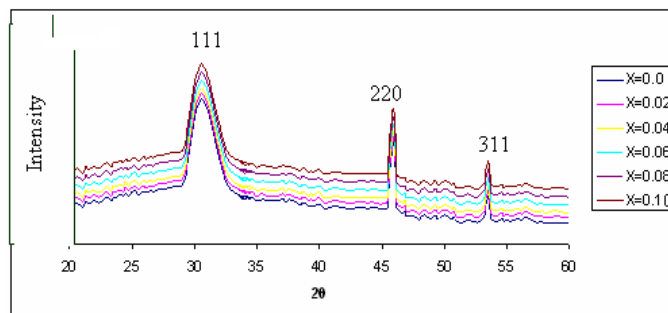


Fig. (7), X- ray pattern for as deposited ZnS_xSe_{1-x} films with thickness 0.5μm annealed at 423 K

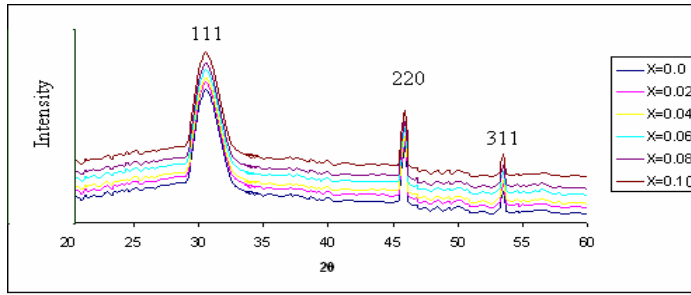


Fig. (8) X- ray pattern for as deposited ZnS_xSe_{1-x} films with thickness $0.7\mu m$.

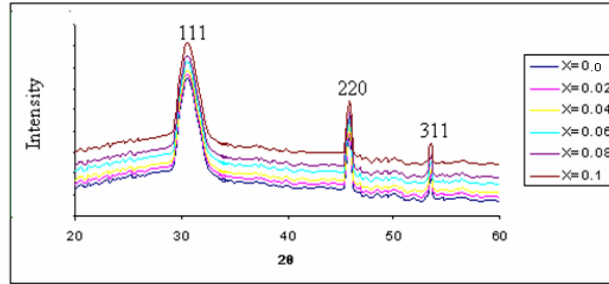


Fig.9, X- ray pattern for as deposited ZnS_xSe_{1-x} films with thickness $0.7\mu m$ annealed at 373 K

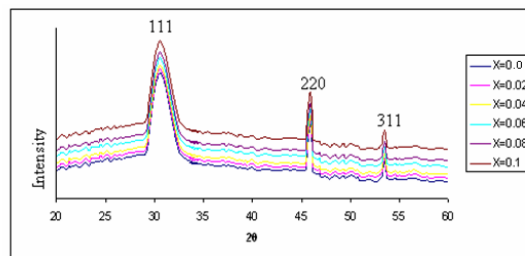


Fig.(10) X- ray pattern for as deposited ZnS_xSe_{1-x} films with thickness $0.7\mu m$ annealed at 423 K

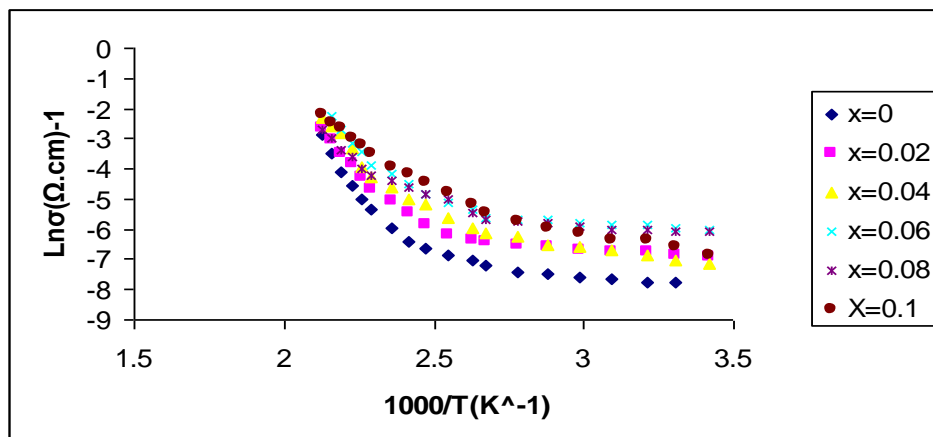


Fig.(11) $Ln\sigma$ as afunction of $10^3/T$ for as deposited $Zn S_xSe_{1-x}$ thin films, at thicknesses $0.3\mu m$.

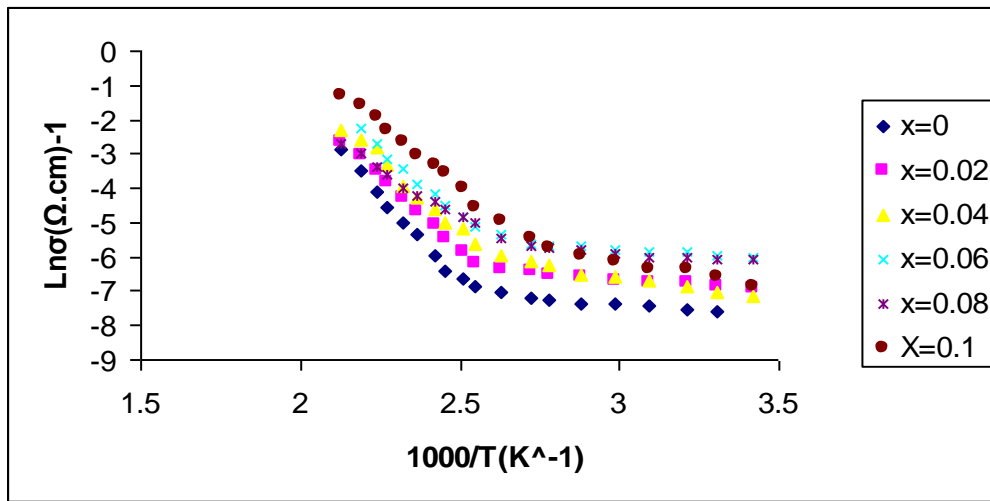


Fig.(12) $\text{Ln}\sigma$ as a function of $10^3/T$ for as deposited $\text{Zn S}_x\text{Se}_{1-x}$ thin films, at thicknesses $0.3\mu\text{m}$ annealed at 373K .

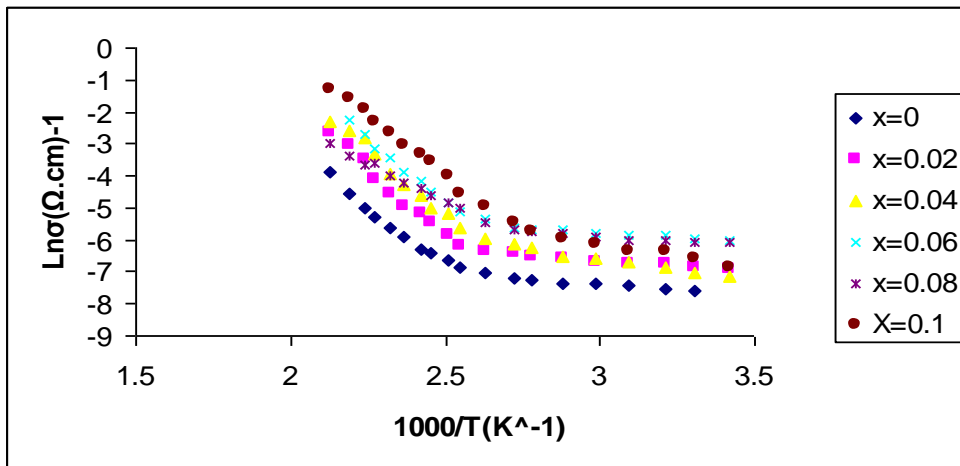


Fig.(13) $\text{Ln}\sigma$ as a function of $10^3/T$ for as deposited $\text{Zn S}_x\text{Se}_{1-x}$ thin films, at thicknesses $0.3\mu\text{m}$ annealed at 423K .

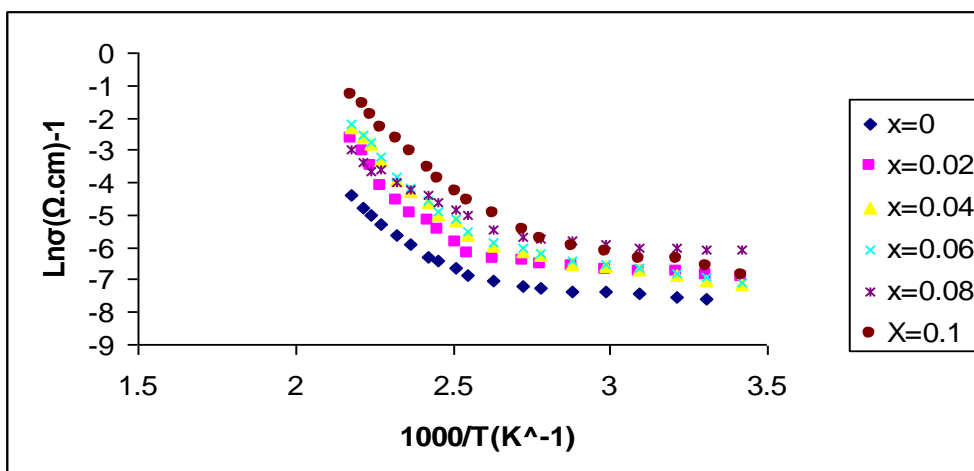


Fig.(14) $\text{Ln}\sigma$ as a function of $10^3/T$ for as deposited $\text{Zn S}_x\text{Se}_{1-x}$ thin films, at thicknesses $0.5\mu\text{m}$.

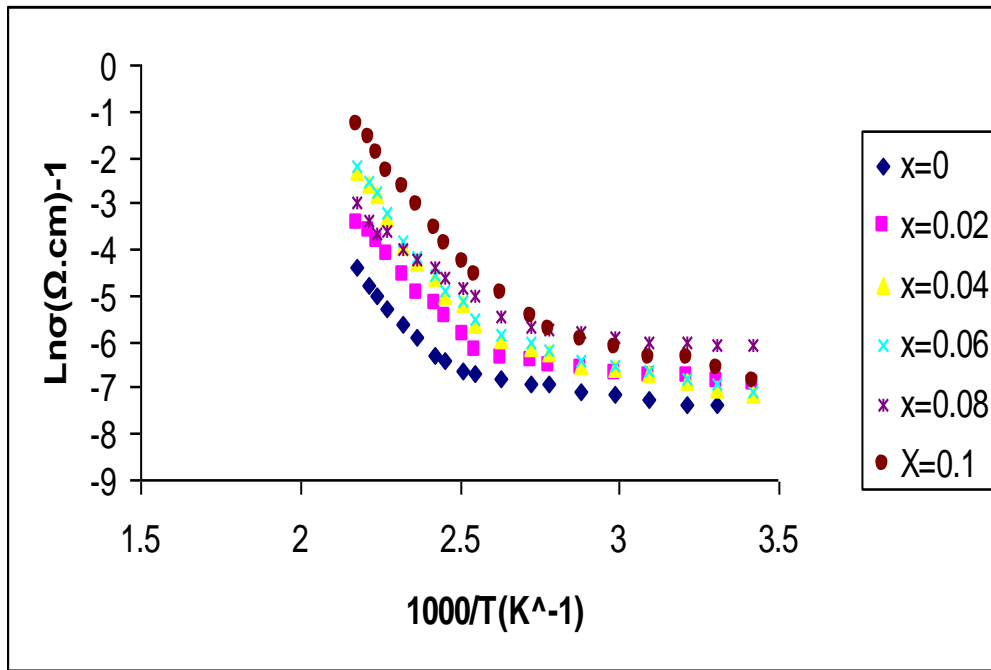


Fig.(15) $Ln\sigma$ as a function of $10^3/T$ for as deposited $Zn S_xSe_{1-x}$ thin films, at thicknesses $0.5\mu m$ annealed at $373K$.

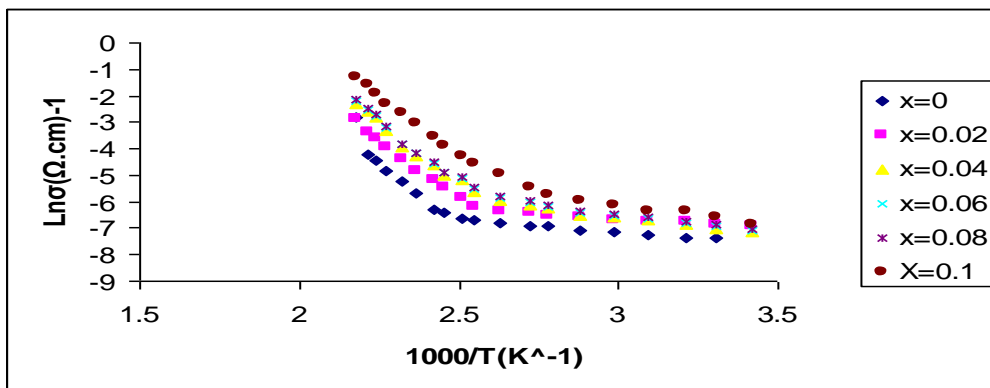


Fig.(16) $Ln\sigma$ as a function of $10^3/T$ for as deposited $Zn S_xSe_{1-x}$ thin films, at thicknesses $0.5\mu m$ annealed at $423K$.

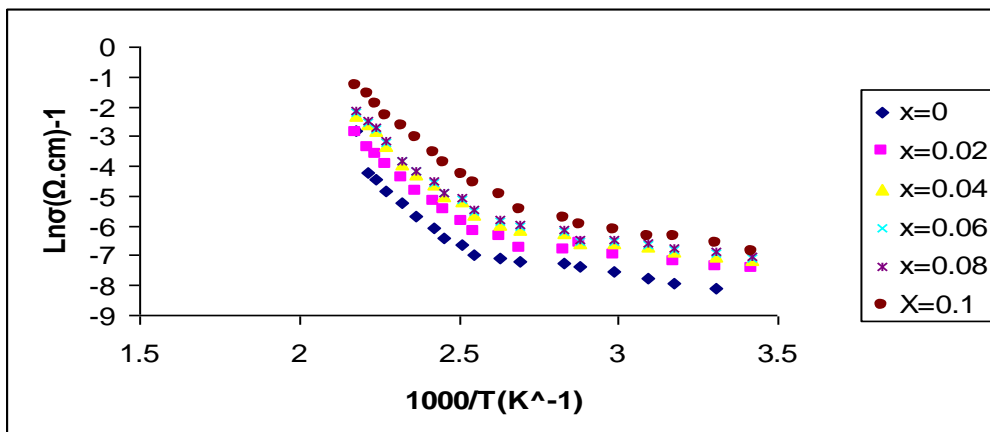


Fig.(17) $Ln\sigma$ as a function of $10^3/T$ for as deposited $Zn S_xSe_{1-x}$ thin films, at thicknesses $0.7\mu m$.

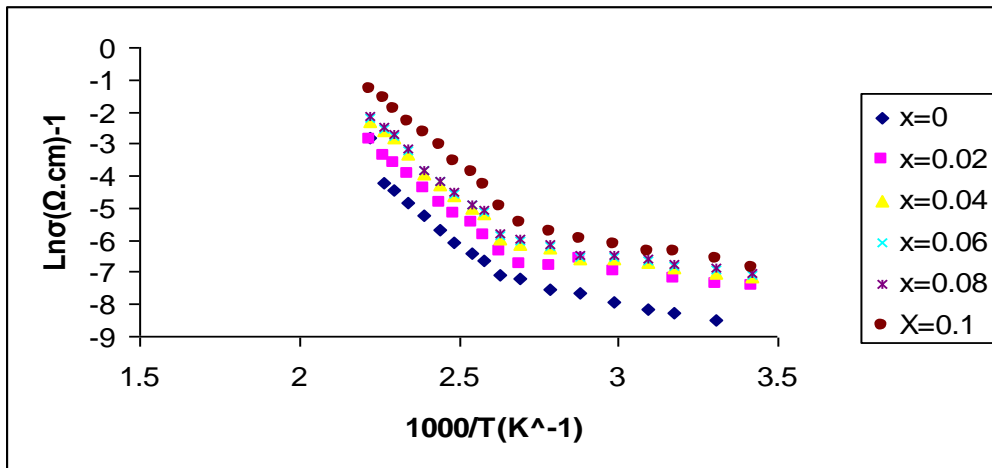


Fig.(18) $\text{Ln}\sigma$ as a function of $10^3/T$ for as deposited $\text{Zn S}_x\text{Se}_{1-x}$ thin films, at thicknesses $0.7\mu\text{m}$ annealed at 373K .

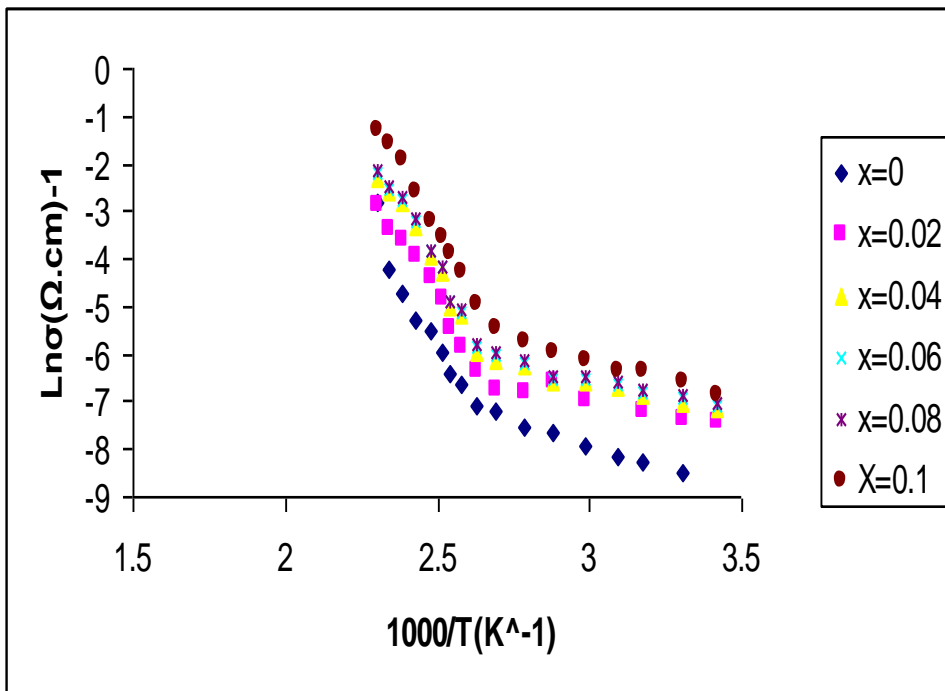


Fig.(19) $\text{Ln}\sigma$ as a function of $10^3/T$ for as deposited $\text{Zn S}_x\text{Se}_{1-x}$ thin films, at thicknesses $0.7\mu\text{m}$ annealed at 423K .

Table (1) D.C. conductivity parameters for ZnS_xSe_{1-x} films at different x and annealing temperatures for thickness 0.3μm.

(x)	$\sigma_{RT} (\Omega.cm)^{-1}$	T _a (K)	Ea ₁ (eV)	Temp.Range (K)	Ea ₂ (eV)	Temp. Range (K)
0.00	3.53*10 ⁻⁷	RT	0.0258	298-333	0.449	333-513
	3.41*10 ⁻⁷	373	0.0461	298-353	0.545	353-513
	3.34*10 ⁻⁷	423	0.0683	298-363	0.627	363-513
0.02	3.38*10 ⁻⁷	RT	0.0269	298-413	0.504	413-513
	3.24*10 ⁻⁷	373	0.0544	298-353	0.655	353-513
	3.18*10 ⁻⁷	423	0.0719	298-383	0.721	383-513
0.04	3.25*10 ⁻⁷	RT	0.0364	298-443	0.596	443-513
	3.14*10 ⁻⁷	373	0.0602	298-433	0.661	433-513
	3.05*10 ⁻⁷	423	0.0723	298-343	0.786	343-513
0.06	3.13*10 ⁻⁷	RT	0.0469	298-353	0.632	353-513
	3.05*10 ⁻⁷	373	0.0647	298-363	0.696	363-513
	2.93*10 ⁻⁷	423	0.0768	298-493	0.812	493-513
0.08	3.02*10 ⁻⁷	RT	0.0512	298-403	0.662	403-513
	2.92*10 ⁻⁷	373	0.0682	298-373	0.723	373-513
	2.81*10 ⁻⁷	423	0.0829	298-383	0.841	383-513
0.10	2.83*10 ⁻⁷	RT	0.0538	298-433	0.699	433-513
	2.52*10 ⁻⁷	373	0.0725	298-353	0.761	353-513
	2.15*10 ⁻⁷	423	0.0933	298-363	0.893	363-513

Table (2) D.C. conductivity parameters for ZnS_xSe_{1-x} films at different x and annealing temperatures for thickness $0.5\mu m$

(x)	$\sigma.d.c$ ($\Omega.cm$) ⁻¹ (R.T)	T _a (K)	Ea ₁ (eV)	Temp. Range (K)	Ea ₂ (eV)	Temp. Range (K)
0.00	$3.63 \cdot 10^{-7}$	RT	0.0249	298-343	0.423	343-513
	$3.50 \cdot 10^{-7}$	373	0.0442	298-363	0.521	363-513
	$3.38 \cdot 10^{-7}$	423	0.0634	298-363	0.613	363-513
0.02	$3.56 \cdot 10^{-7}$	RT	0.0256	298-403	0.492	403-513
	$3.42 \cdot 10^{-7}$	373	0.0526	298-343	0.592	343-513
	$3.36 \cdot 10^{-7}$	423	0.0702	298-383	0.703	383-513
0.04	$3.44 \cdot 10^{-7}$	RT	0.0325	298-453	0.526	453-513
	$3.31 \cdot 10^{-7}$	373	0.0582	298-433	0.632	433-513
	$3.25 \cdot 10^{-7}$	423	0.0711	298-373	0.753	373-513
0.06	$3.34 \cdot 10^{-7}$	RT	0.0432	298-353	0.602	353-513
	$3.25 \cdot 10^{-7}$	373	0.0617	298-353	0.664	353-513
	$3.13 \cdot 10^{-7}$	423	0.0738	298-493	0.792	493-513
0.08	$3.12 \cdot 10^{-7}$	RT	0.0501	298-413	0.625	413-513
	$3.02 \cdot 10^{-7}$	373	0.0645	298-373	0.691	373-513
	$2.92 \cdot 10^{-7}$	423	0.0802	298-383	0.803	383-513
0.10	$2.98 \cdot 10^{-7}$	RT	0.0513	298-433	0.645	433-513
	$2.81 \cdot 10^{-7}$	373	0.0704	298-353	0.723	353-513
	$2.72 \cdot 10^{-7}$	423	0.0912	298-363	0.865	363-513

Table (3) D.C. conductivity parameters for ZnS_xSe_{1-x} films at different x and annealing temperatures for thickness $0.7\mu m$.

(x)	σ_{RT}^{-1} ($\Omega.cm$) ⁻¹	T _a (K)	E _{a1} (eV)	Temp.Range (K)	E _{a2} (eV)	Temp.Range (K)
0.00	3.79×10^{-7}	RT	0.0229	298-353	0.403	353-513
	3.62×10^{-7}	373	0.0421	298-363	0.502	363-513
	3.52×10^{-7}	423	0.0612	298-373	0.592	373-513
0.02	3.73×10^{-7}	RT	0.0237	298-423	0.472	423-513
	3.61×10^{-7}	373	0.0502	298-353	0.561	353-513
	3.48×10^{-7}	423	0.0682	298-383	0.682	383-513
0.04	3.64×10^{-7}	RT	0.0305	298-443	0.501	443-513
	3.53×10^{-7}	373	0.0554	298-433	0.601	433-513
	3.42×10^{-7}	423	0.0698	298-363	0.712	363-513
0.06	3.53×10^{-7}	RT	0.0414	298-353	0.576	353-513
	3.42×10^{-7}	373	0.0587	298-363	0.632	363-513
	3.31×10^{-7}	423	0.0712	298-493	0.761	493-513
0.08	3.28×10^{-7}	RT	0.0481	298-403	0.607	403-513
	3.15×10^{-7}	373	0.0616	298-373	0.662	373-513
	3.03×10^{-7}	423	0.0768	298-383	0.781	383-513
0.10	3.08×10^{-7}	RT	0.0497	298-433	0.625	433-513
	2.98×10^{-7}	373	0.0684	298-353	0.701	353-513
	2.86×10^{-7}	423	0.0878	298-363	0.822	363-513

Table (4) Hall parameters for ZnS_xSe_{1-x} films at different thicknesses and x at temperatures $R.T$

x	t (μm)	$R_H \times 10^4 (\text{cm}^3/\text{C})$	$(n_H) \times 10^{15} \text{cm}^{-3}$	$(\mu_H) \times 10^{-3} (\text{cm}^2/\text{V.s})$
0.00	0.3	8.32	2.94	29.40
	0.5	8.89	2.96	32.30
	0.7	8.81	3.14	33.40
0.02	0.3	8.63	2.79	29.20
	0.5	9.04	2.82	32.20
	0.7	8.79	3.10	32.80
0.04	0.3	8.94	2.74	29.06
	0.5	9.24	2.75	31.80
	0.7	8.55	3.00	32.10
0.06	0.3	9.20	2.59	28.80
	0.5	9.19	2.63	30.70
	0.7	9.15	2.87	31.30
0.08	0.3	9.49	2.56	28.66
	0.5	9.42	2.57	29.40
	0.7	9.20	2.78	30.20
0.10	0.3	10.07	2.53	28.50
	0.5	9.59	2.55	28.60
	0.7	9.54	2.60	29.40

Table (5) Hall parameters for ZnS_xSe_{1-x} films at different thicknesses and x at temperatures $373K$.

x	t (μm)	$R_H \times 10^4 (\text{cm}^3/\text{C})$	$10^{15} \text{cm}^{-3} \times (n_H)$	$10^{-3} (\text{cm}^2/\text{V.s}) \times (\mu_H)$
0.00	0.3	8.32	2.92	28.40
	0.5	8.65	2.94	30.30
	0.7	8.86	3.12	32.10
0.02	0.3	8.70	2.78	28.20
	0.5	8.53	2.80	29.20
	0.7	8.78	3.08	31.70
0.04	0.3	8.93	2.72	28.06
	0.5	8.18	2.73	27.10
	0.7	8.83	2.99	30.20
0.06	0.3	9.11	2.58	27.80
	0.5	7.78	2.60	25.30
	0.7	8.23	2.84	29.30
0.08	0.3	9.47	2.53	27.66
	0.5	8.01	2.55	24.20
	0.7	8.92	2.76	28.10
0.10	0.3	10.91	2.52	27.50
	0.5	8.22	2.53	23.10
	0.7	8.79	2.58	26.20

Table (6) Hall parameters for ZnS_xSe_{1-x} films at different thicknesses and x at temperatures 423K

x	t (μm)	R _H ×10 ⁴ (cm ³ /C)	(n _H)×10 ¹⁵ cm ⁻³	(μ _H)×10 ⁻³ (cm ² /V.s)
0.00	0.3	7.87	2.91	26.31
	0.5	8.31	2.92	28.10
	0.7	8.63	3.10	30.40
0.02	0.3	8.18	2.82	26.02
	0.5	8.09	2.78	27.20
	0.7	8.44	3.06	29.40
0.04	0.3	8.49	2.70	25.92
	0.5	7.78	2.71	25.30
	0.7	7.98	2.97	28.20
0.06	0.3	8.77	2.57	25.71
	0.5	7.69	2.58	24.10
	0.7	8.24	2.82	27.30
0.08	0.3	9.77	2.51	25.52
	0.5	7.97	2.52	23.30
	0.7	8.44	2.74	25.60
0.10	0.3	11.68	2.50	25.13
	0.5	8.23	2.51	22.40
	0.7	8.28	2.56	23.70

Conclusions

According to the above observations, the following conclusion are drawn :- (1) the addition of (S) to ZnSe wide the band gap of the later which consequently decreases the d.c conductivity.(2)the addition of (S) to ZnSe make ($\sigma_{d.c}$) decreases in systematic manner.(3) increasing of T_a and t reduces the states or vacancies in the band gap.(4) ZnSe is n type semiconductor and the addition of(S) to ZnSe films has no effect on the type of conductance.

References

- [1] G.F. Neumark, R.M. Park and M. DePuydt, Phys. Today 47 (1994) 26.
- [2] B. Gil, T. Cloitre, M.D. Blasio, P. Bigenwald, L. Aigouy, N. Briot, O. Briot, D.Bouchara, R.L. Aulombard and J. Calas, Phys. Rev. B 50 (1994) 18231.
- [3] M. Godlewski, E. Guziewicz, K. Kopalko, E. Lusakowska, E. Dynowska, M.M.Godlewski, E.M. Goldys and M.R. Phillips, J. Luminesc. 102 (2003) 455.
- [4] D. Shen, S.Y. Au, G. Han, D. Que, N. Wang and I.K. Sou, J. Mat. Sci. Lett. 22, (2003) 483.
- [5] T. Homann, U. Hotje, M. Binnewies, A. Borger, K.-D. Becker and T. Bredow, Solid State Sci. 8, (2006) 44.
- [6] S.A.B. Nasrallah, N. Sfina, N. Bouarissa and M. Said, J. Phys.: Condens. Matter 18 (2006) 3005.
- [7] F. Janetzko and K. Jug, J. Phys. Chem. A 108 (2004) 5449.
- [8] N. Fitzner, A. Kuligk, R. Redner, M. Stadele, S.M. Goodnick and W. Schattke, Phys. Rev. B 67, (2003) 201201.
- [9] J. Muscat, A. Wander and N.M. Harrison, Chem. Phys. Lett. 342 (2001) 397.
- [10] J.E. Bernard and A. Zunger, Phys. Rev. B 36 (1987) 3199.
- [11] D. Theis, Phys. Stat. Sol. (b), 79, (1977) 125.
- [12] A. Ebina, E. Fukunaka and T. Takahashi, Phys. Rev. B 10, 2495 (1974).
- [13] S.Sze, Physics of Semiconductors Devices, John Wiley and Sons, New York,(2007).
- [14] M.A. Al-Sabayleh, Australian Journal of Basic and Applied Sciences, 3,2 (2009) 669-676.
- [15] Y.Segui, F.Carrere and A.Bui, Thin Solid Films, 92 (1982) 303.
- [16]F. Abdu AL-Hamed Ibraheem, "Study of Some Structural and Electrical Properties of Doped with in of ZnSe Thin Films Properties by Thermal Evaporation" Thesis, Baghdad University, P.42, (2007).